Haptic Tele-cooperation of Multiple Robots

I. Sharifi[1], H. A. Talebi[2], S. A. R. Mousavi [3], and S. Shemshaki[4], M. Tavakoli[5]

***Abstract*— In this paper, a novel haptic tele-cooperation control scheme for a system consisting of multiple manipulators interacting with a physical or virtual object is proposed. The contact force between each manipulator and the object is decomposed into two independent forces, one of which is related to grasping the object and the other is related to the motion of the object including its interaction with the environment it is in. The Lyapunov's direct method is used for designing and stability analysis of the proposed controller. As a case study, the problem of robotic tele-rehabilitation is investigated where multiple human operators (e.g., one or more therapists, patients, and trainees in a tele-rehabilitation setting) control their user interfaces in order to tele-cooperatively manipulate an object in a virtual environment. Experimental results confirm the performance and effectiveness of the proposed control methodology.**

Keywords: Cooperative haptic teleoperation, sliding mode control, tele-rehabilitation.

I. Introduction

Research on cooperative robotic systems has attracted the attention of researchers as these systems are useful for grasping and handling objects of various shapes and weights. There are three main strategies for centralized control of cooperative robots [1]: master-slave control, coordinated motion control, and object motion control. In the master-slave control strategy, one or more robots are considered as the master and others act as the slaves [2]. In the coordinated motion control category, which is the case of this paper, grasping and manipulation of an object are achieved through controlling the robots' end effectors (EEs) [3], [4]. In the object motion control strategy, the system's dynamics are obtained based on the object's dynamic parameters and the object is controlled directly [1], [5].

Several papers have been published on cooperative systems, considering new aspects in the control of these systems [6]–[14]. An experimental study was performed in [6] on a cooperative system consisting of two fully known manipulators handling a rigid object in free motion but the control of the internal forces was not considered in this research. The works in [7] considered cooperative control of two flexible arms of a space robot handling an object. Multiple impedance control (MIC) algorithm and virtual linkages approach was used in [9] to propose a control algorithm for multiple mobile manipulators. The virtual linkages were used for control of the internal forces. An adaptive synchronization architecture for multiple robots with known kinematic parameters was proposed in [12]. In [13] a strategy for motion and internal force control of a cooperative robotic system was developed. However, they did not consider control of contact forces due to the environment-robot interaction.

A control methodology was presented for teleoperation of cooperative systems in [2]. A synchronization method was developed in [15] for cooperative robots in free motion as well as trajectory tracking of the object. The grasping process was also modeled without assuming constraints on contact points. [16] suggested a strategy for position control and synchronization of cooperative robots by introducing the concept of passive decomposition. However, the methodology was *only* developed on point mass mobile robots in free motion.

In this paper, the problem of cooperative grasping of an object with several teleoperated robots is addressed. The system consists of several master haptic interfaces, the same number of slave manipulators, and one object. The slave manipulators and the object can either be physical or virtual. For the virtual case, as each operator works with a robot (haptic master interface), a virtual mirror of that robot (slave robot) interacts with the virtual object in terms of position and force. An important use for such systems is in cooperative therapy for post-disability rehabilitation (see Fig. 1). Accordingly, the case study considered in this paper concerns a tele-rehabilitation scenario. For implementing the VE, a Unity3D© environment [17] is designed.

The rest of paper is organized as follows. In Section II, the reduced order dynamics of the overall system is given in operational space. Our robust adaptive control strategy for both the object's position and the object-environment contact forces is presented in Section III. Control of the internal forces is also covered in this Section. In Section IV, the effectiveness of the proposed controller is verified through experimental results.

II. Dynamic Equations of Motion

In this section, the dynamics of the manipulators, the object and the overall system are given. The following assumptions are made in this work:

(A1) The contact between the end-effector of each robot and the object is rigid.

(A2) The object is rigid.

[1] I. Sharifi is a visiting doctoral student at Department of Electrical and Computer Engineering, University of Alberta, Edmonton, AB, Canada. Email: isharifi@ualberta.ca

[2] H. A. Talebi is with faculty of Electrical Engineering, Amirkabir University of Technology, Tehran, Iran. Email: alit@aut.ac.ir

[3] S. A. R. Mousavi is with the Department of Electrical Engineering, Amirkabir University of Technology, Tehran, Iran. Email: Amousavi@aut.ac.ir

[4] S. Shemshaki is with the Department of Electrical Engineering, Amirkabir University of Technology, Tehran, Iran. Email: ShShemshaki@aut.ac.ir

[5]M. Tavakoli is Professor in Department of Electrical and Computer Engineering, University of Alberta, Edmonton, AB T6G 1H9, Canada. mahdi.tavakoli@ualberta.ca

Fig. 1: Rehabilitation of a patient via cooperative manipulation of a ball together with a therapist [18].

(A3) The rotational speed of the robots' joints and the contact forces between the object and the robots and the objects and its environment are measurable.

(A4) The robots do not get into singular configurations.

A. The Manipulator Dynamics

When the object makes contact with its environment, an impulsive force is exerted on it. This force is generated due to sudden changes in the object's velocity. For simplicity, the effects of this impulsive force are not considered. However, it is possible to consider the impact as a bounded systematic disturbance and to make the controller robust against it.

The dynamic model of each of the manipulators can be expressed as

$$M_i(q_i)\ddot{q}_i + C_i(q_i,\dot{q}_i)\dot{q}_i + g_i(q_i) = \tau_i - J_i^T f_{hi} \tag{1}$$

where $i = 1, 2, ..., r$ and $M_i \in R^{n\times n}$ is the inertia matrix, C_i is the matrix of Coriolis and centrifugal terms, g_i is the vector of gravitational forces, τ_i is the vector of control signals, and f_{hi} is the vector of external forces and moments exerted on the ith manipulator. Moreover, J_i is the analytical Jacobian matrix for the ith robot. The dynamics of the multiple robots are expressed by

$$M_m(q)\ddot{q} + C_m(q,\dot{q})\dot{q} + g_m(q) = \tau - J^T f_h \tag{2}$$

where

$$\begin{aligned} &M_m(q) = diag\{M_i(q_i)\}\ ,\ C_m(q,\dot{q}) = diag\{C_i(q_i,\dot{q}_i)\},\\ &f_h = [f_{h1}^T, \cdots, f_{hr}^T]^T,\ g_m = [g_1^T, \cdots, g_r^T]^T,\\ &\tau = [\tau_1^T, \cdots, \tau_r^T]^T,\ J = diag\{J_i\}\ ;\ i = \{1, ..., r\} \end{aligned}$$

By writing the dynamics of the robots in task space, the following equation is obtained

$$M(X_e)\ddot{X}_e + C(X_e,\dot{X}_e)\dot{X}_e + f_h = u - G(X_e) \tag{3}$$

In this equation, M, C, G and u are the transformed forms of M_m, C_m, g_m and τ defined above, respectively. Moreover, $X_e = [X_{e1}^T, X_{e2}^T, \cdots, X_{er}^T]^T$ denotes the vector of positions of the end-effectors of the manipulators.

B. The Object Dynamics

The dynamics of the object can be written as

$$\begin{aligned} &M_o(X_o)\dot{v}_o + C_o(X_o, v_o)v_o + g_o(X_o) + d_o(t) = f_o\\ &f_o = f_{ho} + f_{co} \end{aligned} \tag{4}$$

where M_o is the inertia matrix, C_o is the matrix of Coriolis and centrifugal terms, g_o is the vector of gravitational forces, d_o is the vector of bounded disturbances exerted on the object (such as friction at the contact point), and f_o is the vector of external forces and moments exerted on the object. The latter consists of two separate terms, namely f_{ho} and f_{co}, which are the external forces and moments of interaction of the object with the robots and the environment, respectively. A diagram of the cooperative system is shown in Figure 2a when the slave manipulators and the object are virtual (a similar arrangement is possible when the slave manipulators and the object are physical).

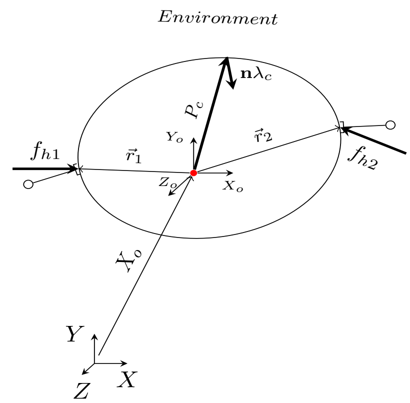

(a) The object in its environment.

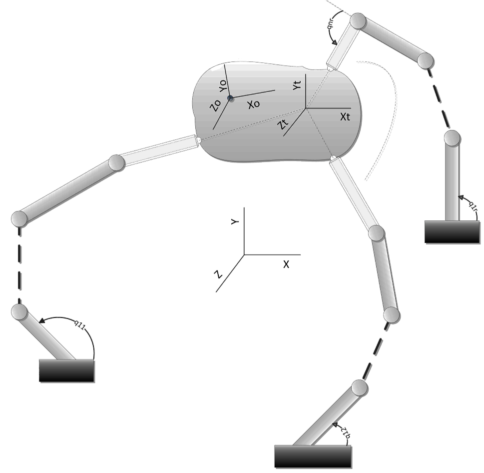

(b) Diagram of the object grasped by the robots.

Fig. 2: Diagram of the manipulated object.

It is noted that $v_o^T = [\dot{\mathbf{x}}_\mathbf{o}^T, \omega^T]$ is the object's velocity in the base coordinate frame ({XYZ}) and

$$f_{ho} = J_o^T f_h\ ,\ \dot{X}_{ei} = J_{oi} v_o \tag{5}$$

in which $J_o = [J_{o1}^T, J_{o2}^T, \cdots, J_{or}^T]^T$ is the so-called grasp matrix. Each grasp matrix between one of the robots' end effectors and the object ($J_{oi}, i = \{1, ..., r\}$), depends on the relative position of the object's centre of mass (COM) and the end-effector of the robot, and it is constant. The interaction forces between the object and the environment are obtained as

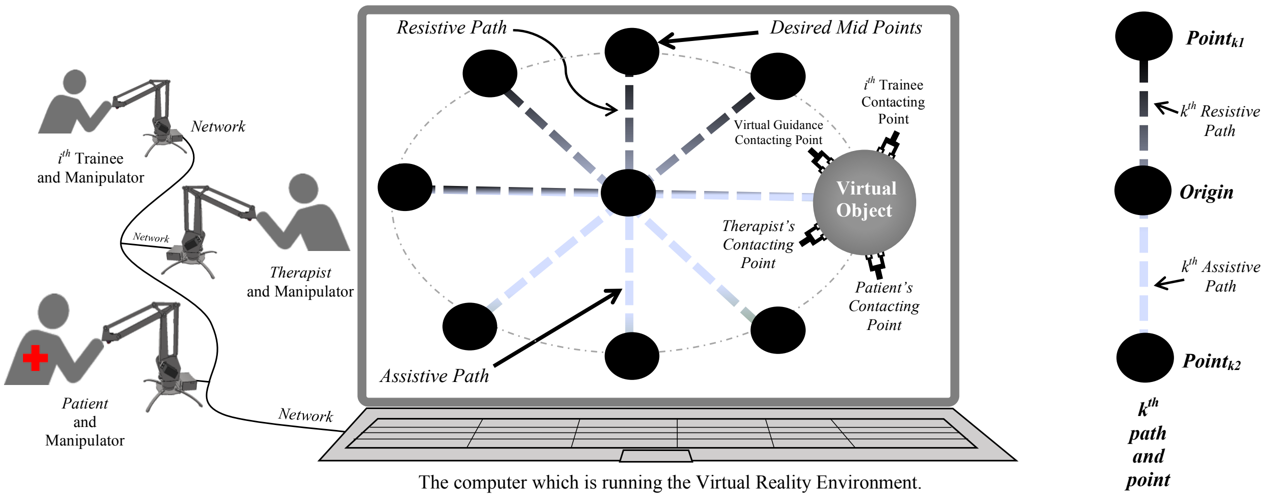

(a) (b)

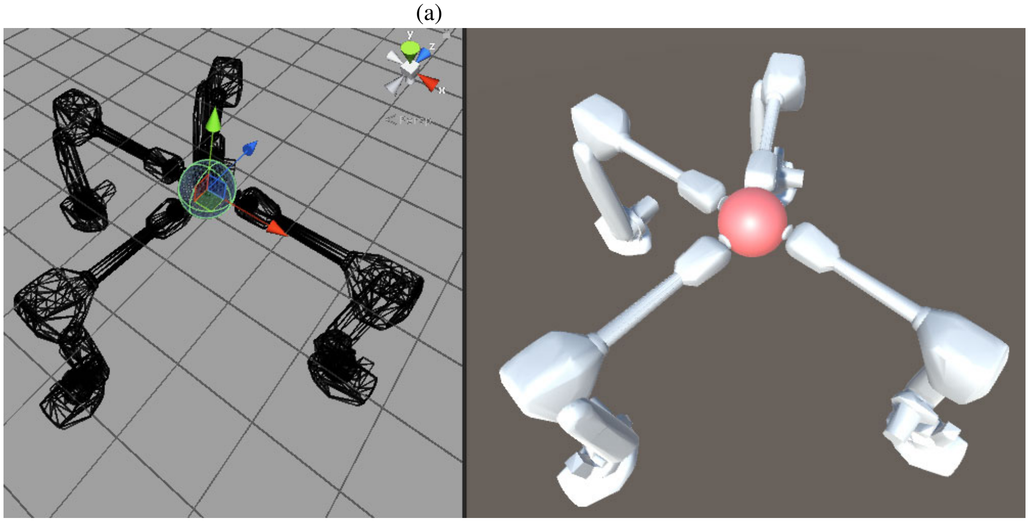

(c) Unity Environment for Virtual Object Manipulation.

Fig. 3: The schematic of the overall system. (a) The schematic which shows the interaction between the operators and the Virtual Realty Environment. The virtual object is touched from different aspects, with therapist, patient, and other operators such as trainees (that are mentioned as the i^{th} operator in the figure). The black circles show the desired mid-points, which the virtual object should reach. The paths are colorized as warm black to cold black, which refer to the resistive to assistive path, respectively. (b) The assistive/resistive paths and points.

$$f_{co} = \begin{bmatrix} \mathbf{n}\lambda_c \\ P_c \times \mathbf{n}\lambda_c \end{bmatrix} = N\lambda_c \tag{6}$$

where $\mathbf{n} \in R^{m\times 1}$ is the unit vector of the exerted force and P_c is a vector connecting the object's coordinate frame origin to the contact point (Figure 2a). $\mathbf{n}$ is known since it depends only on the environment, which is assumed to be known. It is also possible to decompose f_h into two orthogonal subspaces as [19]:

$$f_h = (J_o^T)^\dagger f_{ho} + G_o^{-T} \underbrace{(I - J_I^{\dagger T} J_I^T) f_{hint}}_{F_I} \tag{7}$$

In (7), $G_o = diag\{J_{oi}\}$, $i = \{1, 2, ..., r\}$ and f_{hint} is the vector of internal forces for grasping the object. These forces have no contribution in the object's motion and $J_I = [I_{n\times n}, \cdots, I_{n\times n}]^T \in R^{rn\times n}$. Moreover,

$$\begin{aligned} J_o^T &= J_I^T G_o^T, \\ F_I^T &= [f_{int1}^T, f_{int2}^T, ..., f_{intr}^T], \\ J_I^T F_I &= 0 \end{aligned} \tag{8}$$

Furthermore, f_{inti} is the vector of internal forces between the object and the ith manipulator. $(J_I^T)^\dagger$ is the weighted pseudo inverse of J_I^T defined in (9), in which $Q = diag\{\zeta_i I_{n\times n}\}$, $i = \{1, 2, ..., r\}$, is a matrix that identifies load distribution between the robots:

$$J_I^{\dagger T} = Q J_I (J_I^T Q J_I)^{-1} \tag{9}$$

C. Dynamic Model of the Virtual Fixture

We model the virtual fixture (VF) as another virtual manipulator so that it is general and can have dynamics. In contrast to to the other manipulators, the VF manipulator does not have any mirror in the real world. It is designed to help the patient and the other operators to work in an assistive or a resistive mode of rehabilitation. The dynamic model of the VF can be expressed as

$$M_{vf}(x_{vf})\ddot{x}_{vf} + C_{vf}(x_{vf}, \dot{x}_{vf})\dot{x}_{vf} + \bar{g}_{vf}(x_{vf}) = U_{vf} + F_{\mathrm{e_{vf}}} \tag{10}$$

$$\begin{aligned} U_{vf} = M_{vf}(x_{vf})a_{vf} + C_{vf}(x_{fvf}, \dot{x}_{vf})\dot{x}_{vf} \\ + \bar{g}_{vf}(x_{vf}) - F_{\mathrm{e_{vf}}} \end{aligned} \tag{11}$$

where

$$a_{vf} = \ddot{X}_d - k_1\dot{\tilde{X}}_d - k_2\tilde{X}_d$$

in which

$$X_d(t) = \begin{cases} X_{Origin} & \text{VO is inside resistive path.} \\ X_{Point_2} & \text{VO is inside assistive path.} \end{cases}$$

It is obvious that the derivative of $X_d(t)$ inside the path is zero. So, the internal dynamics become

$$\ddot{X}_{vf}(t) + k_1\dot{X}_{vf}(t) + k_2X_{vf}(t) = X_d$$

where, X_{vf} is the position of the VF, M_{vf} is the inertia matrix, C_{vf} is the matrix of Coriolis and centripetal forces, $\bar{g}_{vf}$ is the vector of gravitational forces, U_{vf} is the vector of control signals and F_{evf} is the vector of human forces exerted on the VF.

D. The Overall Dynamics of the System

According to Assumption A1 and considering the task-space dynamics of the manipulators, the object and the VF in ((3), (4), (7), and (8), the overall dynamics of the cooperative system can be written as

$$M_{x1}\ddot{X}_{e1}+C_{x1}\dot{X}_{e1} = v-T^TG-J_{o1}^{-T}[g_o-N\lambda_c+d_o] \quad (12)$$

where

$$\begin{aligned} M_{x1} &= T^TMT + (J_{o1}^T)^{-1}M_oJ_{o1}^{-1} \\ C_{x1} &= T^TCT + (J_{o1}^T)^{-1}C_oJ_{o1}^{-1} \\ v &= T^Tu = T^Tu_m \end{aligned}$$

and

$$T^T = [I_{6\times6}, T_2^T, \cdots, T_r^T] = constant \\ , \; T_i = J_{oi}J_{o1}^{-1} \; , \; i = \{1, 2, ..., r\}$$

$$T^TF_I = 0 \quad , \quad T^Tu_f = 0$$

As long as the positions of the contact points are known, it can be concluded that the matrix T is constant. This property is used in the controller design. Due to the decoupling of the object's motion and the internal forces exerted on it, it is possible to control each of them independently [19]. Control of the object's motion and the environmental forces exerted on it are performed through designing the signal u_m. Moreover, u_f is the control signal for the internal forces. Therefore, the overall control signal can be obtained as

$$u = u_m + u_f \quad (13)$$

In addition, v is the transformation of the control signal u_m, which is introduced later in Section III. Due to the kinematic constraints between the robots and the object, it is also possible to obtain the overall dynamics of the cooperative system with respect to another point. This point could be the end-effector of another robot or a point on the object such as the geometrical centre of the contact points ((X_t, Y_t, Z_t) in Figure 2b). The following properties can be inferred from (12):

Lemma 1 ([20]): The matrix $\dot{M}_{x1} - 2C_{x1}$ is skew symmetric, i.e.,

$$q^T(\dot{M}_{x1} - 2C_{x1})q = 0 \quad \textit{for every } q \in \mathrm{R}^6$$

Moreover, M_{x1} is symmetric positive definite and is bounded. This means that there exist some positive constants α_{min} and α_{max} such that

$$\alpha_{min}I_{n\times n} \leq M_{x1} \leq \alpha_{max}I_{n\times n}$$

In addition, it can be easily concluded from Lemma 1 that

$$\dot{M}_{x1} = C_{x1} + C_{x1}^T \quad (14)$$

Proposition 1 ([21]): A manipulator with only revolute joints of the form (12) is considered. It is assumed that $\dot{X}_{e1}, \ddot{X}_{e1} \in L_\infty$. Then the derivative terms of its Coriolis matrix, $\dot{C}_{x1}(X_{e1}, \dot{X}_{e1})$, are bounded.

III. Control of the Cooperative System

A. Control of the Object's Motion and the Object-Environment Contact Forces

Manipulators with known dynamic parameters are utilized for handling an object with unknown geometry, inertia, mass and centre of mass position. The grasped object is initially at (x_0, y_0, z_0). Next, the manipulators cooperatively move it so that it makes contact with the environment. Then, the object makes contact with the environment and exerts a controlled force upon it. The following error signals are defined:

$$e = X_{e1} - X_{e1}^d \quad (15)$$

$$e_n = (\lambda_c - \lambda_c^d)\eta \quad (16)$$

In the above, X_{e1}^d and λ_c^d are the desired values of X_{e1} and λ_c, respectively, and $\eta^T = [\mathbf{n}^T, 0_{(n-m)\times1}^T]$. A hybrid force/position control algorithm is defined for controlling the object's motion and its interaction with the environment independently. To this end, the dynamics of the system, (12), are decomposed into two subspaces as

$$S(M_{x1}\ddot{X}_{e1} + C_{x1}\dot{X}_{e1}) = v_p - S(T^TG + J_{o1}^{-T}[g_o - N\lambda_c + d_o]) \quad (17)$$

$$S'(M_{x1}\ddot{X}_{e1} + C_{x1}\dot{X}_{e1}) = v_f - S'(T^TG + J_{o1}^{-T}[g_o - N\lambda_c + d_o]) \quad (18)$$

$$v = v_p + v_f \quad (19)$$

where $v_p = Sv$, $v_f = S'v$. Note that $S(t)$ and $S'(t)$ are the selection matrices that project the dynamics of the system onto the motion and force subspaces, respectively. These diagonal matrices are orthogonal and $S(t) + S'(t) = I_{n\times n}$. The columns of the selection matrices S, S' are the bases of the motion and force subspaces, respectively. Since the control strategy considers both free motion and interaction with the environment as far as the object is concerned, the elements of the selection matrices are time-dependent. In the contact scenario, the diagonal elements of the force subspace selection matrix (S') actually depend on the normal to the environment's surface ($\mathbf{n}$).

In the contact case, since the object is relatively fixed in the exerted force direction, it is assumed that $S'\ddot{X}_{e1} \approx 0$ and $S'\dot{X}_{e1} \approx 0$. Hence (18) is reduced to

$$S'(T^TG + J_{o1}^{-T}[g_o - N\lambda_c + d_o]) = v_f \quad (20)$$

The parameter L is introduced for ease of notation as

$$L = J_{o1}^{-T} N \tag{21}$$

The elements of the selection matrices change only on transition phases from free motion of the object to its contact with the environment. Hyperbolic functions of contact forces are used for making this transition. As a result, time varying elements of $\frac{d}{dt}S(t)$ and $\frac{d}{dt}S'(t)$ are functions of $sech(f(\lambda_c))^2$, which vanishes quickly. Hence, differentiations of the selection matrices are approximated to zero.

Considering Assumptions A3-A4, the control signals are defined as

$$\begin{aligned} v_p &= p(t) - S[K_p s_p + L\lambda_c + d_1 \odot sat(s_p)] \\ v_f &= f(t) - S'[d_1 \odot sat(s_p) - K_f(s_f + e_n)] - \eta\lambda_c^d \end{aligned} \tag{22}$$

where

$$\begin{aligned} p(t) &= S[M_{x1}(\ddot{X}_{e1}^d - \lambda\dot{e}) + C_{x1}(\dot{X}_{e1}^d - \lambda e) \\ &\quad + T^T G + J_{o1}^{-T} g_o] \\ f(t) &= S'[T^T G + J_{o1}^{-T} g_o] \end{aligned} \tag{23}$$

Moreover, $s_p = \dot{e} + \lambda e$ and $s_f = \int_0^t e_n \mathrm{d}\tau$ are the sliding surfaces of the motion and force control subspaces, respectively. In addition, $K_p, K_f \in R^{n\times n}$ are some symmetric positive definite matrices, λ is a positive number and d_1 is an upper bound value for the signal $J_{o1}^{-T} d_o$. Furthermore, $\hat{o}$ means the estimated value of o, $sat(.)$ is the saturation function, and $\odot$ is the symbol of element-wise product. After substituting the control signals (22) into (17) and (20), the error dynamics of the closed loop system are obtained as

$$\begin{aligned} &S[M_{x1}\dot{s}_p + C_{x1}s_p] = S[-K_p s_p - d_1 \odot sat(s_p) - J_{o1}^{-T} d_o] \\ &e_n = (I_{n\times n} + S'K_f)^{-1}[-S'(K_f s_f + d_1 \odot sat(s_f) - J_{o1}^{-T} d_o)] \end{aligned} \tag{24}$$

In addition, (23) can be simplified to

$$\begin{aligned} p(t) &= p_t(t) + p_o(t) \\ p_t(t) &= ST^T J^{-T}[M_m \ddot{q}_t + C_t \dot{q}_t + g_m] \\ p_o(t) &= S[J_{o1}^{-T}(M_o J_{o1}^{-1}\ddot{q}_o + C_o J_{o1}^{-1}\dot{q}_o + g_o)] \end{aligned} \tag{25}$$

Moreover, $\dot{q}_t, \ddot{q}_t, \dot{q}_o$ and $\ddot{q}_o$ are defined as below:

$$\begin{aligned} \dot{q}_t &= J^{-1}T(\dot{X}_{e1}^d - \lambda e) \\ \ddot{q}_t &= J^{-T}T\ddot{X}_{e1}^d - J^{-1}\dot{J}J^{-1}T(\dot{X}_{e1}^d - \lambda e) \end{aligned} \tag{26}$$

$$\begin{aligned} \dot{q}_o &= \dot{X}_{e1}^d - \lambda e \\ \ddot{q}_o &= \ddot{X}_{e1}^d \end{aligned} \tag{27}$$

The main result of the paper is summarized in the following theorem.

Theorem 1: Consider the cooperative system (12) with the control signal (19). Then, the position error e and its derivative converge to zero asymptotically. In addition, the error of the object-environment contact force and e_n remain bounded. Furthermore, if the disturbance signal d_o is differentiable, then $\ddot{e}$ and e_n converge to zero asymptotically.

Proof: The theorem is verified for motion and force subspaces separately.

Motion subspace: The Lyapunov function (28) is used for stability analysis of the motion subspace.

$$V_p = \tfrac{1}{2} s_p^T S M_{x1} s_p \tag{28}$$

Differentiating (28), using (24), and doing some algebraic manipulations, yields

$$\begin{aligned} \dot{V}_p = s_p^T(-S[K_p s_p - d_1 \odot sat(s_p) - J_{o1}^{-T} d_o \\ - C_{x1}s_p + \tfrac{1}{2}\dot{M}_{x1}s_p]) \end{aligned} \tag{29}$$

By using the property (1), it is finally concluded that

$$\dot{V}_p = -s_p^T S K_p s_p - \underbrace{s_p^T S(d_1 \odot sat(s_p) + J_{o1}^{-T} d_o)}_{\geq 0} \leq 0 \tag{30}$$

Hence, $s_p \in L_2 \cap L_\infty$. From (24), property (1) and boundedness of $e, \dot{e}, \dot{X}_{e1}^d, \ddot{X}_{e1}^d, \Omega$ (Ω is a function of the robots and the object parameters), it is concluded that $\ddot{e}$ is bounded. As a result, $e, \dot{e}$ are uniformly continuous. Finally, as a consequence of Barbalat's lemma [22]:

$$\lim_{t\to\infty} e, \dot{e} = 0$$

From (24), it is obtained that

$$\ddot{e} = M_{x1}^{-1}\Psi(e, \dot{e}, e_n, \dot{e}_n, d_o) \tag{31}$$

If the disturbance vector "d_o" is differentiable, then using (14) and the proposition (1), it can be verified that $\frac{d}{dt}\ddot{e}$ which is computed from (32), is bounded

$$\frac{\mathrm{d}}{\mathrm{d}t}\ddot{e} = M_{x1}^{-1}(C_{x1} + C_{x1}^T)M_{x1}^{-1}\Psi + M_{x1}^{-1}\dot{\Psi} \tag{32}$$

Hence, $\ddot{e}$ is uniformly continuous and it is concluded from Barballat's lemma that $\lim_{t\to\infty}\ddot{e} = 0$.

Force subspace: The Lyapunov function (33) is used for stability analysis of the motion subspace.

$$V_f = \frac{1}{2} s_f^T s_f \tag{33}$$

Similarly, differentiating (33), using (24) gives:

$$\dot{V}_f = -s_f^T S' K_f s_f - \underbrace{s_f^T S'(d_1 \odot sat(s_f) + J_{o1}^{-T} d_o)}_{\geq 0} \leq 0$$

As a result, $s_f \in L_2 \cap L_\infty$. From (24) it is concluded that "e_n" is bounded and as a result of Barbalat's lemma "s_f" converges to zero. If the disturbance signal "d_o" is differentiable, differentiating (24) yields that "$\dot{e}_n$" is bounded and uniformly continuous. Finally from Barbalat's lemma "e_n" converges to zero asymptotically and the proof is complete. ■

B. Computation of The Optimal Control Torques

In order to obtain the optimal control torques of the robots, first the control signal "u_m" should be computed from the calculated signal "v" defined in the task space. To this end, the control signals u_{mi} are computed in a way that a cost function $J_u = \frac{1}{2}\sum_{i=1}^r u_{mi}^T u_{mi}$, is minimized with respect to each u_{mi} ($i = \{1, 2, ..., r-1\}$) [23]. Hence, a system of equations is obtained consisting of "r" equations and "r" unknowns:

$$\begin{aligned} &\tfrac{\partial J_u}{\partial u_{mi}} = 0 \quad i = 1, ..., r-1 \\ &v = u_{m1} + \textstyle\sum_{i=2}^r T_i^T u_{mi} \end{aligned} \tag{34}$$

Solving (34), the optimal u_m is obtained. Next, the control signal "u" is computed from (13) and finally the control torques are obtained as:

$$\tau = J^T u \tag{35}$$

C. Internal Force Control

In order to control the internal forces, first they should be computed. Hence, solving (9) results in:

$$J_I^{\dagger T} = [\sigma_1 I_{n\times n}, \cdots, \sigma_m I_{n\times n}]^T \quad (36)$$

where $\sigma_i = \frac{\zeta_i}{\sum_{j=1}^{m} \zeta_j}$ and ζ_i's define the load distribution between the robots. Using (7) and (8), it is verified that:

$$F_I = \begin{bmatrix} J_{o1}^T f_{h1} - \sigma_1 \sum_{i=1}^{r} J_{oi}^T f_{hi} \\ \vdots \\ J_{or}^T f_{h1} - \sigma_r \sum_{i=1}^{r} J_{oi}^T f_{hi} \end{bmatrix} \quad (37)$$

Consequently,

$$f_{inti} = J_{oi}^T f_{hi} - \sigma_i \sum_{j=1}^{r} J_{oj}^T f_{hj} \quad (38)$$

Due to the assumptions (A1) and (A2), the expression "$J_{oi}^{-T} J_{oj}^T$", $\forall i,j \in \{1,2,...,r\}$ depends only on the relative positions between the contact points of the robots and the object. Hence, considering the assumption (A3), the term "F_{int}" defined in (39) is computable based on measurements of the contact forces between the object and the manipulators:

$$F_{int} = G_o^{-T} F_I \in R^{rn\times 1} \quad (39)$$

Now, the control signal u_f is proposed as follows:

$$u_f = F_{intc} = F_{int}^d - \beta(e_{Fint}) \quad (40)$$

where $F_{int}^d = G_o^{-T} F_I^d$ is the vector of desired internal forces and $e_{Fint} = F_{int} - F_{int}^d$ is the internal forces error signal. β is a dynamic control signal which includes integrator operators in time domain. It should be noted that no derivatives of the internal forces are used in (40). For example, (41) can be suggested as a definition of β, in which K_1, K_2 and K_3 are some positive definite matrices:

$$\beta = K_1 e_{Fint} + K_2 \int_0^t e_{Fint}\, d\rho + K_3 \int_0^t \int_0^t e_{Fint}\, d\rho \quad (41)$$

Theorem 2: Consider the cooperative system (3), with the control signal (13), then the errors for the internal forces remain bounded. Moreover, if the disturbance signal d_o is differentiable, these errors converge to zero.

Proof: For simplicity, it is assumed that β in (40) is defined as (41). By substituting (13) into the dynamic equation of motion (3), the error dynamics of the internal forces are obtained as

$$e_{Fint} + K_1 e_{Fint} + K_2 \int_0^t e_{Fint}\, d\rho + K_3 \int_0^t \int_0^t e_{Fint}\, d\rho = -\varphi(t) \quad (42)$$

where

$$\begin{aligned} \varphi(t) = F_{intc} - F_{int} = M\ddot{X}_e + C\dot{X}_e + G - u_m \\ - J_o^{\dagger T}(M_o \ddot{X}_o + C_o \dot{X}_o + g_o + d_o - f_{co}) \end{aligned} \quad (43)$$

According to the results of the Theorem 1, $(e, \dot{e}, \ddot{e}, e_n)$ and their derivatives are limited. Thus, $\varphi(t) \in Ł_\infty$ and as a result, e_{Fint} remains bounded. Moreover, as long as e, $\dot{e}$, $\ddot{e}$, e_n and $\dot{e}_n$ converge to zero and the disturbance signal d_o is differentiable, $\varphi(t)$ will converge to a constant vector. Now, suppose that $B(s) = \mathcal{L}\beta(t)$ is of type one or higher, *i.e.* $B(s) = \frac{1}{s}\Delta(s)$, which $\Delta(s) \in RH_\infty$ is a stable transfer function. It is then concluded from the final value theorem that:

$$\lim_{t\to\infty} e_{Fint}(t) = \lim_{s\to 0} sE_{Fint}(s) = \lim_{s\to 0} \frac{s^2}{\Delta(s)} \Phi(s) = 0$$

For example, considering $\beta(t)$ as (41):

$$E_{Fint}(s)(\frac{K_2}{s} + (1 + K_1) + \frac{K_3}{s^2}) = \frac{\Phi(s)}{s}$$

Hence, using the final value theorem it is obtained that:

$$\lim_{t\to 0} e_{Fint}(t) = \lim_{s\to 0} \frac{s^2}{s^2(1+K_1) + sK_2 + K_3} \Phi(s) = 0$$

■

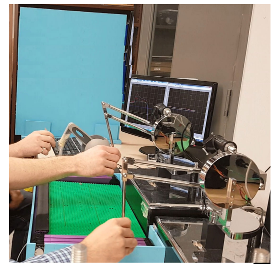

Fig. 4: The operators who are working as the Therapist, the Patient, and the Trainee.

IV. Experimental Results

In order to illustrate the performance of the proposed method, an experimental tele-rehabilitation system is developed. In this system, there are four operators consisting of a therapist, a patient, a trainee, who are working with Phantom Premium/Omni devices (Fig. 4). Beside a VF is utilized as the fourth operator in VF as depicted in Fig. 3a. In this figure, the darker paths show the resistive directions while the paler paths show the assistive directions as far as the effect of the VF on the object movement is concerned. The operators are working with 6-DOF Phantom Premium devices as the manipulators. The 3D dynamical and graphical models of the manipulators are built in Unity3D. Likewise, a virtual ball is designed inside the virtual environment (see Fig. 3c). Furthermore, the controller is implemented in Simulink Desktop Real-Time™ [24] and its input/output is connected to Unity3D via the UDP protocol. Fig. 5 shows the results for experimentation. As illustrated in Figures 5a and 5b, the system starts working in resistive mode. After 120 seconds, the system goes to assistive mode. In the assistive mode ($>$ 120 seconds), due to the presence of the assistive VF force, the forces applied by the human operators on their respective manipulators decrease. In the resistive mode ($<$ 120 seconds), due to the presence of the VF resistive force, the forces applied by the human operators on their respective manipulators increase to be able to move the object. The 2D position of the ball is depicted in Fig. 6.

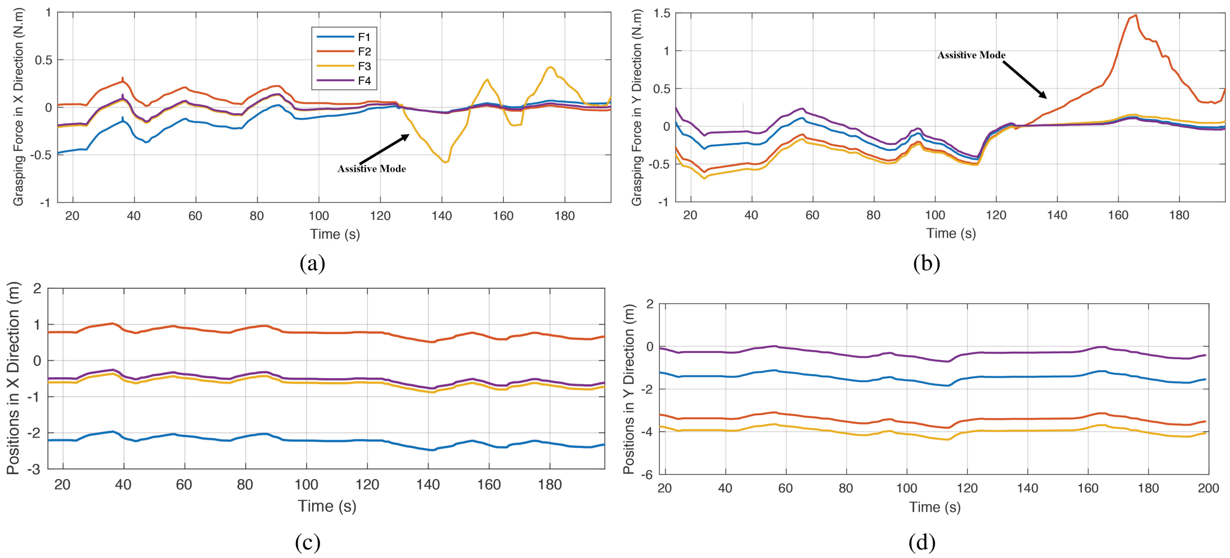

Fig. 5: After 120 seconds the system goes to assistive mode and the Virtual Guidance Manipulator's force help others to move.

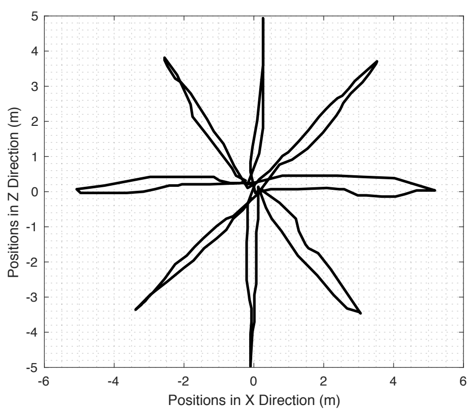

Fig. 6: 2D position of Virtual Ball.

References

[1] S. Schneider and R. H. Cannon, "Object impedance control for cooperative manipulation," in *Proceedings of IEEE International Conference on Robotics and Automation*. IEEE, 1989, pp. 1076–1083.

[2] S. Sirouspour, "Modeling and control of cooperative teleoperation systems," *IEEE Transactions on Robotics*, vol. 21, no. 6, pp. 1220–1225, December 2005.

[3] P. Pagilla and M. Tomizuka, "Hybrid force/motion control of two arms carrying an object," in *Proceedings of the American Control Conference*, June 1994, pp. 195–199.

[4] W. Gueaieb, S. Al-Sharhan, and M. Bolic, "Robust computationally efficient control of cooperative closed-chain manipulators with uncertain dynamic," *Automatica*, pp. 842 – 851, 2007.

[5] Z. Li, S. Ge, and Z. Wang, "Robust adaptive control of coordinated multiple mobile manipulators," *Mechatronics*, vol. 13, pp. 239–250, 2008.

[6] J. Gudino-Lau and M. Arteaga, "Dynamic model and simulation of cooperative robots: a case study," *Robotica*, vol. 23, pp. 615–624, 2005.

[7] S. Liu, L. Wu, and Z. Lu, "Impact dynamics and control of a flexible dual-arm space robot capturing an object," *Applied Mathematics and Computation*, vol. 185, pp. 1149–1159, 2007.

[8] H. Xie, I. J. Bryson, F. Shadpey, and R. V. Patel, "A robust control scheme for dual-arm redundant manipulators: experimental results," in *Proceedings 1999 IEEE International Conference on Robotics and Automation (Cat. No.99CH36288C)*, vol. 4, 1999, pp. 2507–2512 vol.4.

[9] R. Rastegari and S. A. Moosavian, "Multiple impedance control of space free-flying robots via virtual linkages," *Acta Astronautica*, vol. 66, pp. 748–759, 2010.

[10] M. Yamano, J. Kim, A. Konno, and M. Uchiyama, "Cooperative control of a 3d dual-flexible-arm robot," *Journal of Intelligent and Robotic Systems*, vol. 39, pp. 1–15, 2004.

[11] J. Martinez-Rosas, M. Arteaga, and A. Castillo-Sanchez, "Decentralized control of cooperative robots without velocity-force measurements," *Automatica*, vol. 42, pp. 329–336, October 2006.

[12] W. Zhu, "On adaptive synchronization control of coordinated multirobots with flexible/rigid constraints," *IEEE Transactions on Robotics*, vol. 21, no. 3, pp. 520–525, June 2005.

[13] R. Tinos, M. Terra, and J. Ishihara, "Motion and force control of cooperative robotic manipulators with passive joints," *IEEE Transactions on Control Systems Technology*, vol. 14, no. 4, pp. 725–734, July 2006.

[14]

[15] D. Sun and J. Mills, "Adaptive synchronized control for coordination of multi-robot assembly tasks," *IEEE Transactions on Robotics and Automation*, vol. 18, no. 4, pp. 498–510, August 2002.

[16] D. Lee, O. Martinez-Palafox, and M. Spong, "Bilateral teleoperation of multiple cooperative robots over delayed communication networks: application." Proceedings of IEEE International Conference on Robotics and Automation, April 2005, pp. 366–371.

[17] L. Wang, D. Johnson, and Y. Lin, "Improving a roundabout design through simulation in a unity 3d virtual environment," in *Advances in Human Aspects of Transportation*. Springer, 2017, pp. 219–228.

[18] "Ball rehabilitation scheme." http://towncentrerehab.com/service/neurological-rehabilitation, accessed: 2017-02-26.

[19] J. Wang, S. J. Dodds, and W. N. Bailey, "Co-ordinated control of multiple robotic manipulators handling a common object - theory and experiments," *IEE Proc.-Control Theory Appl.*, vol. 144, no. 1, pp. 73–84, January 1997.

[20] Z. Li, W. Chen, and J. Luo, "Adaptive compliant force/motion control of coordinated non-holonomic mobile manipulators interacting with unknown non-rigid environments," *Neuro-computing of Science Direct*, pp. 1330–1344, 2008.

[21] E. Nuno, L. Basanez, R. Ortega, and M. Spong, "Position tracking for non-linear teleoperators with variable time delay," *The International Journal of Robotics Research*, vol. 27, no. 8, pp. 895–910, July 2009.

[22] K. Narendra and A. Annaswamy, *Stable adaptive systems*. Prentice-Hall international, 1989.

[23] P. Pagilla and M. Tomizuka, "Adaptive control of two robot arms carrying an unknown object," in *Proceedings of the IEEE Conference on Robotics and Automation*, 1995, pp. 597–602.

[24] O. N. Sahin, E. Uzunoglu, E. Tatlicioglu, and M. Dede, "Design and development of an educational desktop robot r3d," *Computer Applications in Engineering Education*, 2017.